

**Kinetic Investigation of Translesion Synthesis across a 3-Nitrobenzanthrone-Derived DNA
Lesion Catalyzed by Human DNA Polymerase Kappa**

Kenneth K. Phi^{†,‡}, Madison C. Smith^{†,‡}, E. John Tokarsky^{§,‡}, and Zucai Suo^{§,⊥,*}

[†]*Department of Chemistry and Biochemistry, §The Ohio State Biophysics Program, The Ohio State University, Columbus, OH 43210, USA.* [⊥]*Department of Biomedical Sciences, Florida State University College of Medicine, Tallahassee, FL 32306, USA.*

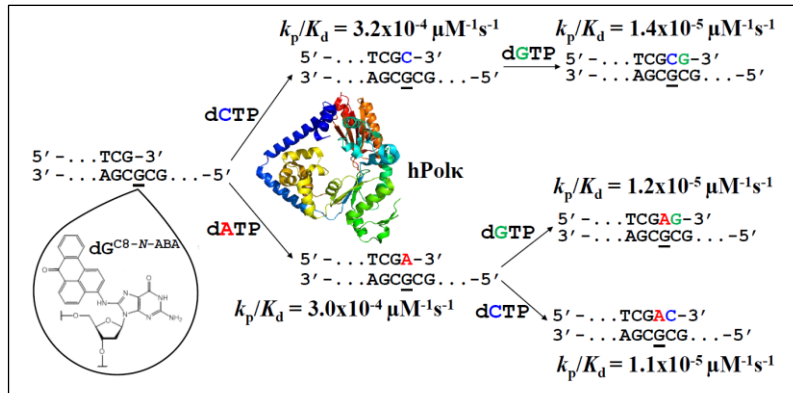
[‡]Authors contributed equally

*To whom correspondence should be addressed: Department of Biomedical Sciences, Florida State University College of Medicine, 1115 West Call Street, Tallahassee, FL 32306-4300. Tel. (850) 645-2501. Email address: zucai.suo@med.fsu.edu.

Keywords:

3-Nitrobenzathrone, Translesion synthesis, Human DNA polymerase kappa, DNA lesion bypass, DNA lesion bypass product extension, and DNA repair.

Table of Contents Graphic (3.33 in. by 1.88 in.):



ABSTRACT

3-Nitrobenzanthrone (3-NBA) is a byproduct of diesel exhaust and is highly present in industrial and populated areas. Inhalation of 3-NBA results in formation of *N*-(2'-deoxyguanosin-8-yl)-3-aminobenzanthrone ($dG^{C8-N-ABA}$), a bulky DNA lesion that is of concern due to its mutagenic and carcinogenic potential. If $dG^{C8-N-ABA}$ is not bypassed during genomic replication, the lesion can stall cellular DNA replication machinery, leading to senescence or apoptosis. We have previously used running start assays to demonstrate that human DNA polymerases eta (hPol η) and kappa (hPol κ) are able to catalyze translesion DNA synthesis (TLS) across a site-specifically placed $dG^{C8-N-ABA}$ in a DNA template. Consistently, gene knockdown of hPol η and hPol κ in HEK293T cells reduces the efficiency of TLS across $dG^{C8-N-ABA}$ by ~25 and ~30%, respectively. Here, we kinetically investigated why hPol κ paused when bypassing and extending from $dG^{C8-N-ABA}$. Our kinetic data show that correct dCTP incorporation efficiency of hPol κ dropped by 116-fold when opposite $dG^{C8-N-ABA}$ relative to undamaged dG, leading to hPol κ pausing at the lesion site observed in the running start assays. The already low nucleotide incorporation fidelity of hPol κ was further decreased by 10-fold during lesion bypass and thus, incorrect nucleotides, especially dATP, were incorporated opposite $dG^{C8-N-ABA}$ with comparable efficiencies as correct dCTP. With regard to the $dG^{C8-N-ABA}$ bypass product extension step, hPol κ incorporated correct dGTP onto the damaged DNA substrate with a 786-fold lower efficiency than onto the corresponding undamaged DNA substrate, resulting in hPol κ pausing at the site in the running start assays. Furthermore, hPol κ extended the primer-terminal matched base pair dC:d $G^{C8-N-ABA}$ with a 100-1,000 fold lower fidelity than it extended the undamaged dC:dG base pair. Together, our kinetic results strongly indicate that hPol κ was error-prone during TLS of $dG^{C8-N-ABA}$.

INTRODUCTION

Genomic DNA is constantly exposed to endogenous and exogenous chemical agents that can damage DNA bases and form a myriad of DNA lesions. Most lesions cause significant problems during DNA replication by stalling replicative DNA polymerases, leading to polymerase switching and erroneous DNA synthesis. 3-Nitrobenzanthrone (3-NBA), a nitrated polycyclic aromatic hydrocarbon produced by incomplete combustion of diesel fuel, is a carcinogenic chemical found in high levels in industrial areas.¹ This chemical has been ranked as one of the most mutagenic chemicals based on the Ames *Salmonella typhimurium* (TA98) assay results.¹ Upon inhalation, 3-NBA is biochemically modified into a metabolite that reacts with DNA bases to form DNA adducts including the major product *N*-(2'-deoxyguanosin-8-yl)-3-aminobenzanthrone (dG^{C8-N-ABA}) (Figure 1).² The dG^{C8-N-ABA} lesion is produced by the electrophilic attack of deoxyguanosine by the metabolite *N*-OH-ABA yielded from sequential nitroreduction and acylation of 3-NBA (Figure 1). After exposure to a low dosage of 3-NBA, bioactivation in human cells can occur within 30 minutes and cause altered gene expression.³⁻⁴ Also, dG^{C8-N-ABA} has been shown to inhibit the activities of various human DNA polymerases *in vitro* and stall DNA replication fork in human cells.⁵⁻⁶

Replicative DNA polymerases are responsible for faithful genome replication due to both their tight polymerase active sites that select for correct base pairing during DNA polymerization and their associated 3' to 5' exonuclease domains that proof read newly incorporated nucleotides.⁷⁻⁹ Upon encountering DNA lesions, replicative DNA polymerases are stalled which can lead to replication fork uncoupling and collapse as well as eventual cell death.¹⁰ To rescue stalled DNA

replication, cells use a DNA damage tolerance pathway known as translesion DNA synthesis (TLS) to cope with DNA lesions. TLS is often catalyzed by Y-family DNA polymerases based on their capabilities of accommodating DNA lesions into their flexible active sites.¹¹ Relative to replicative DNA polymerases, the Y-family polymerases have much lower nucleotide incorporation fidelity and do not possess the 3' to 5' exonuclease domains. Thus, the Y-family DNA polymerases must be regulated by cells to prevent excessive mutagenesis during TLS.¹²⁻¹³ In humans, there are four lesion bypass Y-family DNA polymerases including eta (hPol η), kappa (hPol κ), iota (hPol ι), and Rev1.^{5, 14} These polymerases possess different lesion bypass specificities and distinct kinetic properties.⁸

Previously, our running start assays have shown that among the human Y-family polymerases, only hPol η and hPol κ efficiently bypass a site-specifically placed dG^{C8-N-ABA} lesion in a DNA template.⁵ We have employed pre-steady state kinetics to determine nucleotide incorporation efficiency and fidelity at and adjacent to the dG^{C8-N-ABA} site and establish a minimal kinetic mechanism for TLS of dG^{C8-N-ABA} catalyzed by hPol η .⁵ However, it is mechanistically unclear how hPol κ catalyzes TLS of dG^{C8-N-ABA}. In this study, we performed pre-steady-state kinetic investigation of dG^{C8-N-ABA} bypass and subsequent extension of the lesion bypass products by hPol κ . The kinetic parameters determined for the two steps of TLS help establish a kinetic basis for polymerase pausing and low nucleotide incorporation fidelity at the two sites. The potential *in vivo* roles of hPol κ in TLS of dG^{C8-N-ABA} were discussed.

MATERIALS AND METHODS

Materials

All reagents were purchased from the following companies: OptiKinase from United States Biochemical, [γ -³²P] ATP from Perkin-Elmer, Biospin-6 columns from Bio-Rad Laboratories, and dNTPs from Bioline. Truncated hPolk fragments (9-518) were overexpressed and purified as previously described.¹⁵

DNA substrates

The 26-mer DNA template (26-mer-dG^{C8-N-ABA}, Table 1), containing a site-specifically placed dG^{C8-N-ABA} lesion at position 21, was synthesized as previously described¹⁶ and kept in dark conditions to preserve its chemical integrity. Other synthetic oligonucleotides in Table 1 were purchased from Integrated DNA Technologies (IDT) and purified via a 17% denaturing polyacrylamide gel electrophoresis (PAGE). Primers were 5'-radiolabeled by incubating with OptiKinase and [γ -³²P] ATP in the OptiKinase buffer for 3 hours at room temperature. This was followed by heat inactivation of the kinase (95 °C for 5 min), removal of unreacted [γ -³²P] ATP using a Biospin 6 column (Bio-Rad), and measurement of the radioactivity of each primer in a scintillation counter. The 5'-radiolabeled primer was annealed to a template at 1:1.35 molar ratio by mixing the oligonucleotides and promptly heating the mixture to 95 °C for the undamaged 26-mer template (Table 1), or 72 °C for 26-mer-dG^{C8-N-ABA} for 5 min, followed by slowly cooling the mixture to 25 °C for several hours.

Reaction buffer and product analysis

Kinetic assays were performed by using a Rapid Chemical Quench-Flow apparatus (KinTek) at 37 °C in buffer R (50 mM HEPES, pH 7.5, 50 mM NaCl, 5 mM MgCl₂, 0.1 mM EDTA, 10% glycerol, 5 mM DTT, and 0.1 mg/mL BSA). All reported concentrations were final upon mixing. Reaction products were separated via 17% PAGE (8M Urea, 1X TBE) and quantitated via a TyphoonTrio phosphorimager (GE Healthcare). Software Kaleidagraph (Synergy) was used to perform non-linear regression data analysis.

Single-turnover kinetic assays

A pre-incubated solution of 5'-[³²P]-labeled DNA (30 nM) and hPolκ (300 nM) in buffer R was mixed with varying concentrations of a dNTP (25 to 2000 μM) for various times before being quenched with 0.37 M EDTA. After reaction mixtures were separated and quantitated, product concentration was plotted against reaction time and each plot was fit to a single exponential equation. (Eq. 1)

$$[\text{Product}] = A[1 - \exp(-k_{\text{obs}}t)] \quad (1)$$

Where A is the reaction amplitude and k_{obs} is the observed nucleotide incorporation rate constant. The k_{obs} values were then plotted against dNTP concentration and the plot was fit to a hyperbolic equation. (Eq. 2)

$$k_{\text{obs}} = k_p[\text{dNTP}] / ([\text{dNTP}] + K_{d, \text{dNTP}}) \quad (2)$$

Where k_p is the maximum nucleotide incorporation rate and the $K_{d, \text{dNTP}}$ is the apparent equilibrium dissociation constant of the dNTP.

RESULTS

Inefficient and error-prone bypass of dG^{C8-N-ABA} by hPolk.

In our previously published running start assays,⁵ we have demonstrated that hPolk is able to bypass a site-specifically placed dG^{C8-N-ABA} lesion in the template 26-mer-dG^{C8-N-ABA} (Table 1) although this lesion bypass polymerase is moderately stalled when bypassing the lesion and subsequently extending the lesion bypass products (intense bands of 20-mer and 21-mer in Figure S1). It takes hPolk 7 s (t_{50}^{bypass}) to elongate 50% of the intermediate product 20-mer to 21-mer with template 26-mer-dG^{C8-N-ABA}, which is 23-fold longer than the corresponding t_{50} of 0.3 s obtained with the control template 26-mer (Figure S1).⁵ To explore the mechanistic basis for hPolk pausing during dG^{C8-N-ABA} bypass, we performed single-turnover kinetic assays and determined kinetic parameters for single nucleotide incorporation opposite dG^{C8-N-ABA}. For example, a preincubated solution of hPolk (300 nM) and 5'-[³²P]-labeled 20/26-mer-dG^{C8-N-ABA} (30 nM) was mixed with varying concentrations of dCTP (25-2000 μ M) in buffer R (Materials and Methods) at 37 °C for various times before being quenched with 0.37 M EDTA. At a specific dCTP concentration, the plot of product concentration versus reaction time was fit to Eq. 1 (Materials and Methods) to obtain observed nucleotide incorporation rate constant (k_{obs}) (Figure S2). The k_{obs} values were then plotted against dCTP concentrations and the plot was fit to Eq. 2 (Materials and Methods) to obtain a maximal nucleotide incorporation rate constant (k_p) of $(5.5 \pm 1.0) \times 10^{-1} \text{ s}^{-1}$ and an apparent equilibrium dissociation constant ($K_{d,\text{dCTP}}$) of $1710 \pm 563 \mu\text{M}$ for dCTP binding (Figure 2B), resulting in a calculated dCTP incorporation efficiency ($k_p/K_{d,\text{dNTP}}$) of $3.2 \times 10^{-4} \mu\text{M}^{-1}\text{s}^{-1}$ (Table 2). Relative to our previously published kinetic parameters for dCTP incorporation opposite undamaged dG in the control DNA substrate 20/26-mer (Table 1),¹⁷ dG^{C8-N-ABA} lowered dCTP binding affinity by 37-fold on the basis of the $K_{d,\text{dCTP}}$ difference

(46 *versus* 1710 μ M), decreased dCTP incorporation rate constant (k_p) by 3-fold (1.7 *versus* 0.55 s^{-1}), and reduced dCTP incorporation efficiency ($k_p/K_{d,dNTP}$) by 116-fold (3.7×10^{-2} *versus* $3.2 \times 10^{-4} \mu M^{-1}s^{-1}$) (Table 2).

To examine if hPolk is error-prone when bypassing dG^{C8-N-ABA}, we performed similar single-turnover kinetic assays to those in Figures S2 and 2B and obtained kinetic parameters for each incorrect nucleotide incorporation opposite dG^{C8-N-ABA} (Table 2). When opposite the lesion, hPolk incorporated incorrect dATP (Figure 2C), dGTP (data not shown), and dTTP (data not shown) with comparable values of k_p ($1.0 \times 10^{-2} - 1.5 \times 10^{-1} s^{-1}$), $K_{d,dNTP}$ ($223 - 1147 \mu M$), and $k_p/K_{d,dNTP}$ ($4.5 \times 10^{-5} - 3.0 \times 10^{-4} \mu M^{-1}s^{-1}$) (Table 2). Relative to corresponding kinetic parameters for incorrect nucleotide incorporation opposite undamaged dG in the 20/26-mer (Table 1) measured previously,¹⁷ the k_p value was reduced by 5.4-fold, on average, and the $K_{d,dNTP}$ value was increased by 1.2-fold, on average, leading to a 6.5-fold decrease of the $k_p/K_{d,dNTP}$ value, on average, for incorrect dNTP incorporation opposite dG^{C8-N-ABA} (Table 2). Interestingly, opposite dG^{C8-N-ABA}, the calculated probability of correct dCTP incorporation (43.5%) was only slightly higher than 40.8% for dATP misincorporation and is lower than the total misincorporation probability (56.5%) (Table 2), indicating that hPolk bypassed dG^{C8-N-ABA} in a very error-prone manner. Consistently, the calculated low fidelity ($(1.6 - 2.9) \times 10^{-2}$) of hPolk with the control 20/26-mer was further decreased by 12-fold, on average, with 20/26-mer-dG^{C8-N-ABA} ($(1.2 - 4.8) \times 10^{-1}$, Table 2). Therefore, our kinetic data indicate that dG^{C8-N-ABA} bypass catalyzed by hPolk is highly mutagenic. This is not unexpected considering that hPolk has previously been found to inaccurately bypass similar guanine lesions that fit its active site.¹⁸⁻¹⁹

Extension of a primer-terminal matched junction base-pair dC:dG^{C8-N-ABA} by hPolk.

Our running start assays show that hPolk moderately paused when extending dG^{C8-N-ABA} bypass products as indicated by the accumulation of the intermediate product 21-mer (Figure S1).⁵ To understand why hPolk paused during the first extension step, similar single-turnover kinetic assays to those in Figures S2 and 2B were performed to determine kinetic parameters (Table 3) for individual nucleotide incorporation onto 5'-[³²P]-labeled-21-dC/26-mer-dG^{C8-N-ABA} containing the primer-terminal matched junction base pair dC:dG^{C8-N-ABA} (Table 1). Figure 3 shows a sample gel image of dNTP incorporation onto 5'-[³²P]-labeled-21-dC/26-mer-dG^{C8-N-ABA}. Opposite the templating nucleotide dC, hPolk incorporated correct dGTP with a k_p of $(1.1 \pm 0.1) \times 10^{-2} \text{ s}^{-1}$, a $K_{d,\text{dGTP}}$ of $770 \pm 248 \text{ } \mu\text{M}$, and a $k_p/K_{d,\text{dGTP}}$ of $1.4 \times 10^{-5} \text{ } \mu\text{M}^{-1}\text{s}^{-1}$ (Table 3). Relative to the corresponding kinetic parameters of dGTP incorporation onto the control DNA substrate 21-dC/26-mer (Table 1),¹⁷ the k_p was lowered by 90-fold while the $K_{d,\text{dNTP}}$ was increased by ~9-fold, leading to a 786-fold reduction of dGTP incorporation efficiency with 21-dC/26-mer-dG^{C8-N-ABA} than with 21-dC/26-mer (Table 3). In addition, Table 3 also shows that individual incorrect nucleotides were incorporated onto 21-dC/26-mer-dG^{C8-N-ABA} with comparable k_p values (3.3×10^{-4} to $1.8 \times 10^{-3} \text{ s}^{-1}$), $K_{d,\text{dNTP}}$ values ($140 - 824 \text{ } \mu\text{M}$), and $k_p/K_{d,\text{dNTP}}$ values (1.4×10^{-6} to $2.4 \times 10^{-6} \text{ } \mu\text{M}^{-1}\text{s}^{-1}$). The average $k_p/K_{d,\text{dNTP}}$ for incorrect nucleotides was 24-fold lower with 21-dC/26-mer-dG^{C8-N-ABA} ($2.0 \times 10^{-6} \text{ } \mu\text{M}^{-1}\text{s}^{-1}$) than with 21-dC/26-mer ($4.9 \times 10^{-5} \text{ } \mu\text{M}^{-1}\text{s}^{-1}$), but the decrease is much less dramatic than the 786-fold drop measured for correct dGTP. These $k_p/K_{d,\text{dNTP}}$ differences contribute to calculated nucleotide incorporation fidelity and probability values (Table 3). In comparison, the calculated probability for correct dGTP incorporation is 70.4% with 21-dC/26-mer-dG^{C8-N-ABA} and 98.6% with 21-dC/26-mer while the average fidelity of hPolk is 30-fold lower with the damaged (1.3×10^{-1}) than with the control DNA substrate (4.4×10^{-3}).

Thus, the extension of 21-dC/26-mer-dG^{C8-N-ABA} is also error-prone but less dramatic than dG^{C8-N-ABA} bypass by hPolk (Tables 2 and 3).

Extension of primer-terminal mismatched junction base pairs dN:dG^{C8-N-ABA} and dN:dG by hPolk.

Previously, hPolk has been proposed to be the polymerase to catalyze primer extension from primer-terminal mismatched junction base pairs during DNA replication and TLS.²⁰⁻²³ When bypassing dG^{C8-N-ABA}, hPolk misincorporates dATP, dGTP, and dTTP with probabilities of 40.8, 9.6, and 6.1%, respectively (Table 2), suggesting that subsequently, this Y-family polymerase more frequently extends incorrectly over the correctly bypassed products. To kinetically examine if hPolk is able to catalyze mismatch extension on DNA substrates containing dG^{C8-N-ABA}, we performed single-turnover kinetic assays as described above for correct dGTP and incorrect dCTP incorporation and the measured kinetic parameters are listed in Table 4. For example, three sample gel pictures in Figure 3 illustrate a few time points for each dNTP incorporation onto an indicated 5'-[³²P]-labeled-DNA substrate. Figure S3 shows how we determined k_{obs} , k_p , and $K_{d,dNTP}$ values for correct dGTP incorporation onto 5'-[³²P]-labeled-21-dT/26-mer-dG^{C8-N-ABA}. Notably, all mismatch extensions with correct dGTP on the DNA substrates containing dG^{C8-N-ABA} were relatively inefficient with $k_p/K_{d,dNTP}$ values in the range of $2.7 \times 10^{-6} - 3.2 \times 10^{-5}$ $\mu\text{M}^{-1}\text{s}^{-1}$ (Table 4), which is surprisingly comparable to the $k_p/K_{d,dNTP}$ of dGTP incorporation (1.4×10^{-5} $\mu\text{M}^{-1}\text{s}^{-1}$, Table 3) obtained with the extension of the matched junction base pair dC:dG^{C8-N-ABA}. Thus, hPolk does not favor primer-terminal matched over mismatched junction base pairs when extending dG^{C8-N-ABA} bypass products in the presence of correct dGTP.

For the extension of mismatched junction base pair dG:dG^{C8-N-ABA}, the k_p and $K_{d,dNTP}$ for incorrect dCTP incorporation by hPolκ (Table 4) was measured to be $(1.1 \pm 0.1) \times 10^{-1} \text{ s}^{-1}$ and $1608 \pm 331 \text{ } \mu\text{M}$, respectively. In comparison, correct dGTP was incorporated with a 35-fold slower k_p ($(3.1 \pm 0.6) \times 10^{-3} \text{ s}^{-1}$) and a 1.4-fold smaller $K_{d,dNTP}$ ($1155 \pm 501 \text{ } \mu\text{M}$). Overall, the efficiency of extending dG:dG^{C8-N-ABA} with incorrect dCTP ($6.8 \times 10^{-5} \text{ } \mu\text{M}^{-1} \text{ s}^{-1}$) is 25-fold more efficient with correct dGTP ($2.7 \times 10^{-6} \text{ } \mu\text{M}^{-1} \text{ s}^{-1}$), indicating that hPolκ preferred incorrect over correct dNTP when extending the junction base pair dG:dG^{C8-N-ABA}.

In regard to the extension of the mismatched junction base pair dT:dG^{C8-N-ABA}, hPolκ incorporated correct dGTP with a k_p of $(3.2 \pm 0.1) \times 10^{-3} \text{ s}^{-1}$, a $K_{d,dNTP}$ of $101 \pm 16 \text{ } \mu\text{M}$, and a calculated $k_p/K_{d,dNTP}$ of $3.2 \times 10^{-5} \text{ } \mu\text{M}^{-1} \text{ s}^{-1}$ (Table 4). In comparison, hPolκ incorporated incorrect dCTP with a 97-fold lower $k_p/K_{d,dNTP}$ ($3.3 \times 10^{-7} \text{ } \mu\text{M}^{-1} \text{ s}^{-1}$, Table 4) than correct dGTP. We did not determine k_p and $K_{d,dNTP}$ for dCTP misincorporation because its k_{obs} versus [dCTP] plot could be fit to a linear equation ($k_{obs} = m[\text{dCTP}] + \text{constant}$), where $m = k_p/K_{d,dNTP}$, rather than Eq. 2 (Materials and Methods).

As for the extension of the mismatched junction base pair dA:dG^{C8-N-ABA} by hPolκ, correct dGTP incorporation and dCTP misincorporation have similar k_p , $K_{d,dNTP}$, and $k_p/K_{d,dNTP}$ values (Table 4). Interestingly, both correct ($k_p/K_{d,dNTP} = 1.2 \times 10^{-5} \text{ } \mu\text{M}^{-1} \text{ s}^{-1}$) and incorrect ($k_p/K_{d,dNTP} = 1.1 \times 10^{-5} \text{ } \mu\text{M}^{-1} \text{ s}^{-1}$) elongation of dA:dG^{C8-N-ABA} are as efficient as correct extension of dC:dG^{C8-N-ABA} ($k_p/K_{d,dNTP} = 1.4 \times 10^{-5} \text{ } \mu\text{M}^{-1} \text{ s}^{-1}$, Table 3). Considering that hPolκ incorporated correct dCTP and incorrect dATP opposite dG^{C8-N-ABA} with similarly high probabilities (Table 2), this enzyme efficiently elongated both dA:dG^{C8-N-ABA} and dC:dG^{C8-N-ABA} during the second step of TLS.

To investigate if the error-prone nature of hPolk during the elongation of above mismatched junction base pairs dN:dG^{C8-N-ABA} was due to dG^{C8-N-ABA}, we determined the kinetic parameters (Table 4) for both correct dGTP and incorrect dCTP incorporation onto undamaged primer-terminal junction base pairs dN:dG. All undamaged mismatch extension was similarly inefficient with $k_p/K_{d,dNTP}$ values in the range of $2.7 \times 10^{-6} - 9.5 \times 10^{-4} \mu M^{-1}s^{-1}$ for correct dGTP and $2.1 \times 10^{-6} - 7.6 \times 10^{-5} \mu M^{-1}s^{-1}$ for dCTP misincorporation, leading to a low fidelity in the range of $5.5 \times 10^{-1} - 7.4 \times 10^{-2}$ (Table 4). Furthermore, these $k_p/K_{d,dNTP}$ and fidelity values are comparable to those corresponding ones obtained with dN:dG^{C8-N-ABA} mismatch extension, suggesting the presence of dG^{C8-N-ABA} had little effect on the error-prone mismatch extension nature of hPolk.

DISCUSSION

Kinetic basis for hPolk pausing during dG^{C8-N-ABA} bypass and subsequent extension.

Cells utilize TLS in order to bypass a multitude of different DNA lesions during genomic replication, and the Y-family DNA polymerases, such as hPolk, are the main polymerases to catalyze this process *in vivo*. For example, gene knockdown of hPolk decreases the TLS extent of a single dG^{C8-N-ABA} in a plasmid by ~30% in human embryonic kidney 293T cells.²² Here, we mechanistically investigated how hPolk traverses a site-specifically placed, mutagenic dG^{C8-N-ABA} lesion *in vitro* by performing pre-steady-state kinetic analysis. Previously, our running start assays (Figure S1) have shown that hPolk is able to bypass dG^{C8-N-ABA} in the template 26-mer-dG^{C8-N-ABA} and subsequently extend the lesion bypass products, and that hPolk clearly pauses after the synthesis of the intermediate products 20-mer and 21-mer with the damaged relative to the undamaged template.⁵ To establish a kinetic basis for polymerase pausing, we employed single-turnover kinetic assays to determine nucleotide incorporation efficiency ($k_p/K_{d,dNTP}$) with the damaged and undamaged DNA substrates. Our results indicate that during the lesion bypass step, hPolk incorporated correct dCTP onto 20/26-mer-dG^{C8-N-ABA} with 116-fold lower $k_p/K_{d,dNTP}$ than it incorporated correct dCTP onto the control substrate 20/26-mer (Table 2), and that during the first elongation step, hPolk incorporated correct dGTP onto 21/26-mer-dG^{C8-N-ABA} with 786-fold lower $k_p/K_{d,dNTP}$ than it incorporated correct dGTP onto the control substrate 21/26-mer (Table 3). Moreover, the $k_p/K_{d,dNTP}$ values for incorrect dNTP incorporation during the lesion bypass and subsequent extension steps are either smaller or comparable to those of corresponding correct nucleotide incorporations (Tables 2 and 3). The $k_p/K_{d,dNTP}$ differences coupled with lower k_p values and higher $K_{d,dNTP}$ values for correct nucleotide incorporation onto

damaged over undamaged DNA substrates (Tables 2 and 3) contributed to the strong accumulation of the intermediate products 20-mer and 21-mer and hPolk pausing at these positions (Figure S1). Notably, a similar kinetic basis has previously been established by us for polymerase pausing during TLS of dG^{C8-N-ABA} by hPol η ⁵ and for TLS of N-(deoxyguanosin-8-yl)-1-aminopyrene (dG^{AP}) by hPol η , hPolk, and hPol ι .¹⁷ Thus, human Y-family DNA polymerases likely utilize a common kinetic basis to catalyze TLS of bulky DNA lesions.⁸

Error-prone TLS of dG^{C8-N-ABA} by human polymerase kappa

During dG^{C8-N-ABA} bypass, hPolk has a low fidelity of $(1.2 - 4.8) \times 10^{-1}$, which is 10-fold lower than the fidelity of $(1.6 - 2.9) \times 10^{-2}$ with the undamaged DNA substrate 20/26-mer (Table 2). Consequently, hPolk has a higher probability of incorporating incorrect nucleotides (total 56.5%) over correct dCTP (43.5%, Table 2), leading to the formation of lesion bypass products containing both matched and mismatched junction base pairs which will be the DNA substrates for subsequent extension by hPolk. Notably, the probabilities of incorrect dATP (40.8%) and correct dCTP incorporation opposite dG^{C8-N-ABA} are comparable (Table 2), indicating that hPolk predominantly misincorporated dATP during dG^{C8-N-ABA} bypass. If the *in vitro* observation occurs *in vivo*, it will result in G → T mutation. This scenario is supported by the fact that G → T is the most common mutation during the replication of a plasmid containing a single dG^{C8-N-ABA} in human embryonic kidney 293T cells.²² Furthermore, the probabilities of dNTP incorporation opposite dG^{C8-N-ABA} (Table 2) indicate that dC:dG^{C8-N-ABA} and dA:dG^{C8-N-ABA} are the main primer-terminal junction base pairs to be extended during the next step of TLS by hPolk.

For the extension of the matched junction base pair dC:dG^{C8-N-ABA}, hPolk has a low fidelity in the range of $(0.91 - 1.5) \times 10^{-1}$ which is slightly higher than the fidelity of dG^{C8-N-ABA} bypass (Table 2) but is 100-fold lower than nucleotide incorporation fidelity with the control DNA substrate 21/26-mer (Table 2). Unlike the dG^{C8-N-ABA} bypass step, hPolk preferentially incorporated correct dGTP (70.4% probability) over incorrect dNTPs (Table 3).

Among the three mismatched junction base pairs, dA:dG^{C8-N-ABA} (Fidelity = 0.48) and dG:dG^{C8-N-ABA} (Fidelity = 0.96) were extended by hPolk with a 5-9 fold lower fidelity than it extended dC:dG^{C8-N-ABA} ($(0.91 - 1.5) \times 10^{-1}$) (Tables 3 and 4). Only the extension of the mismatched junction base pair dT:dG^{C8-N-ABA} (1.0×10^{-2}) has a 10-fold higher fidelity but it has the lowest probability (6.1%) to be generated during dG^{C8-N-ABA} bypass (Table 2). Based on the low fidelity values determined with both dG^{C8-N-ABA} bypass and subsequent extension, we conclude that TLS of dG^{C8-N-ABA} catalyzed by hPolk is error-prone, a likely mechanism for which 3-NBA promotes tumorigenesis.²⁴⁻²⁵

Potential Roles of hPolk during TLS of dG^{C8-N-ABA} in vivo

Previously, we have demonstrated that hPol η and hPolk are capable of bypassing dG^{C8-N-ABA} *in vitro* while primer elongation catalyzed by hPol ι and Rev1 are inhibited dramatically, although not completely, by the bulky lesion.⁵ We have also determined that hPol η incorporates dCTP onto 20/26-mer-dG^{C8-N-ABA} with a $k_p/K_{d, \text{dNTP}}$ of $5.8 \times 10^{-3} \mu\text{M}^{-1}\text{s}^{-1}$,⁵ which is 18-fold higher than hPolk incorporates dCTP onto the same DNA substrate ($3.2 \times 10^{-4} \mu\text{M}^{-1}\text{s}^{-1}$) (Table 5). In addition, although we did not determine DNA binding affinity here, our previous work has shown that hPolk binds DNA (undamaged or damaged) weakly with much lower affinity than hPol η .¹⁷

Taken together, we speculate that hPol η is likely the main polymerase to bypass dG^{C8-N-ABA} *in vivo* while hPol κ plays a backup role. During the first lesion bypass product extension step, hPol η incorporates correct dGTP onto 21/26-mer-dG^{C8-N-ABA} with a $k_p/K_{d,dNTP}$ of $2.9 \times 10^{-2} \mu M^{-1}s^{-1}$ ^{1,5}, which is 2,071-fold higher than the elongation efficiency of hPol κ with a matched ($1.4 \times 10^{-5} \mu M^{-1}s^{-1}$, Table 5) or 906-10,740 fold higher than mismatched ($(0.27 - 3.2) \times 10^{-5} \mu M^{-1}s^{-1}$, Table 4) junction base pair dN:dG^{C8-N-ABA}. Considering their different affinities towards DNA, these kinetic data suggest that hPol η can efficiently extend its lesion bypass products and does not need the help of hPol κ . This is inconsistent with a previously proposed polymerase-switching model (dG^{C8-N-ABA} bypassing by hPol η and subsequent extension by hPol κ) for error-prone TLS of dG^{C8-N-ABA}.²² However, hPol η and hPol κ likely catalyze TLS as components of cellular DNA replication machinery containing other proteins factors, *e.g.* proliferating cell nuclear antigen, which may alter the functional significance of these Y-family DNA polymerases in DNA lesion bypass *in vivo*. Thus, our biochemical studies cannot be used to unambiguously determine cellular role of hPol η and hPol κ in TLS of dG^{C8-N-ABA} that requires more studies, especially *in vivo* studies.

Interestingly, the extension of matched and mismatched junction base pairs by hPol κ has comparable $k_p/K_{d,dNTP}$ values (10^{-5} to $10^{-6} \mu M^{-1}s^{-1}$) with the 26-mer-dG^{C8-N-ABA} and 26-mer templates (Tables 3 and 4), suggesting that hPol κ is capable of extending mismatched base pairs²¹ and such an ability is independent of the presence of dG^{C8-N-ABA}. In contrast, hPol η extends primer-terminal matched base pairs with 100-1,000 fold higher efficiencies than mismatched base pairs.²¹ Thus, hPol κ likely acts as a primary primer-terminal mismatch extension polymerase under the polymerase-switching model of TLS.^{23, 25-26}

Funding

This work was supported by the National Science Foundation (grant number MCB-1716168) and the National Institutes of Health (grant number GM124177) to Z.S.

Acknowledgements

We sincerely thank Ashis K. Basu at University of Connecticut for providing us the DNA oligonucleotide 26-mer-dG^{C8-N-ABA}.

Abbreviations

TLS, Translesion synthesis; 3-NBA, 3-nitrobenzathrone; hPol κ , Human DNA Polymerase Kappa; hPol η , Human DNA Polymerase Eta.

Conflict of interest statement: The authors declare that there are no conflicts of interest.

Supporting Information: Figures S1-S3 are included in the Supporting Information. Figure S1 – hPol κ running start assays, Figure S2 – kinetic plots for dCTP incorporation time courses at different dCTP concentrations, Figure S3 – single-turnover kinetic assays for dGTP incorporation onto 21-dT/26-mer-dG^{C8-N-ABA}.

References

1. Arlt, V. M., 3-Nitrobenzanthrone, a potential human cancer hazard in diesel exhaust and urban air pollution: a review of the evidence. *Mutagenesis* **2005**, *20* (6), 399-410.
2. Arlt, V. M.; Phillips, D. H.; Reynisson, J., Theoretical investigations on the formation of nitrobenzanthrone-DNA adducts. *Org Biomol Chem* **2011**, *9* (17), 6100-10.
3. Pink, M.; Verma, N.; Zerries, A.; Schmitz-Spanke, S., Dose-Dependent Response to 3-Nitrobenzanthrone Exposure in Human Urothelial Cancer Cells. *Chem Res Toxicol* **2017**, *30* (10), 1855-1864.
4. Kucab, J. E.; Zwart, E. P.; van Steeg, H.; Luijten, M.; Schmeiser, H. H.; Phillips, D. H.; Arlt, V. M., TP53 and lacZ mutagenesis induced by 3-nitrobenzanthrone in Xpa-deficient human TP53 knock-in mouse embryo fibroblasts. *DNA Repair (Amst)* **2016**, *39*, 21-33.
5. Tokarsky, E. J.; Gadkari, V. V.; Zahurancik, W. J.; Malik, C. K.; Basu, A. K.; Suo, Z., Pre-steady-state kinetic investigation of bypass of a bulky guanine lesion by human Y-family DNA polymerases. *DNA Repair (Amst)* **2016**, *46*, 20-28.
6. Kawanishi, M.; Fujikawa, Y.; Ishii, H.; Nishida, H.; Higashigaki, Y.; Kanno, T.; Matsuda, T.; Takamura-Enya, T.; Yagi, T., Adduct formation and repair, and translesion DNA synthesis across the adducts in human cells exposed to 3-nitrobenzanthrone. *Mutat Res* **2013**, *753* (2), 93-100.
7. Johansson, E.; Dixon, N., Replicative DNA polymerases. *Cold Spring Harb Perspect Biol* **2013**, *5* (6).
8. Maxwell, B. A.; Suo, Z., Recent insight into the kinetic mechanisms and conformational dynamics of Y-Family DNA polymerases. *Biochemistry* **2014**, *53* (17), 2804-14.
9. Raper, A. T.; Reed, A. J.; Suo, Z., Kinetic Mechanism of DNA Polymerases: Contributions of Conformational Dynamics and a Third Divalent Metal Ion. *Chem Rev* **2018**, *118* (12), 6000-6025.
10. Lehmann, A. R.; Niimi, A.; Ogi, T.; Brown, S.; Sabbioneda, S.; Wing, J. F.; Kannouche, P. L.; Green, C. M., Translesion synthesis: Y-family polymerases and the polymerase switch. *DNA Repair (Amst)* **2007**, *6* (7), 891-9.
11. Kunkel, T. A., DNA replication fidelity. *J Biol Chem* **2004**, *279* (17), 16895-8.
12. Sekimoto, T.; Oda, T.; Kurashima, K.; Hanaoka, F.; Yamashita, T., Both high-fidelity replicative and low-fidelity Y-family polymerases are involved in DNA rereplication. *Mol Cell Biol* **2015**, *35* (4), 699-715.
13. Prakash, S.; Johnson, R. E.; Prakash, L., Eukaryotic translesion synthesis DNA polymerases: specificity of structure and function. *Annu Rev Biochem* **2005**, *74*, 317-53.
14. Taggart, D. J.; Fredrickson, S. W.; Gadkari, V. V.; Suo, Z., Mutagenic potential of 8-oxo-7,8-dihydro-2'-deoxyguanosine bypass catalyzed by human Y-family DNA polymerases. *Chem Res Toxicol* **2014**, *27* (5), 931-40.
15. Sherrer, S. M.; Fiala, K. A.; Fowler, J. D.; Newmister, S. A.; Pryor, J. M.; Suo, Z., Quantitative analysis of the efficiency and mutagenic spectra of abasic lesion bypass catalyzed by human Y-family DNA polymerases. *Nucleic Acids Res* **2011**, *39* (2), 609-22.
16. Gadkari, V. V.; Tokarsky, E. J.; Malik, C. K.; Basu, A. K.; Suo, Z., Mechanistic investigation of the bypass of a bulky aromatic DNA adduct catalyzed by a Y-family DNA polymerase. *DNA Repair (Amst)* **2014**, *21*, 65-77.

17. Sherrer, S. M.; Sanman, L. E.; Xia, C. X.; Bolin, E. R.; Malik, C. K.; Efthimiopoulos, G.; Basu, A. K.; Suo, Z., Kinetic analysis of the bypass of a bulky DNA lesion catalyzed by human Y-family DNA polymerases. *Chem Res Toxicol* **2012**, 25 (3), 730-40.

18. Ohashi, E.; Ogi, T.; Kusumoto, R.; Iwai, S.; Masutani, C.; Hanaoka, F.; Ohmori, H., Error-prone bypass of certain DNA lesions by the human DNA polymerase kappa. *Genes Dev* **2000**, 14 (13), 1589-94.

19. Zhang, Y.; Yuan, F.; Wu, X.; Wang, M.; Rechkoblit, O.; Taylor, J. S.; Geacintov, N. E.; Wang, Z., Error-free and error-prone lesion bypass by human DNA polymerase kappa in vitro. *Nucleic Acids Res* **2000**, 28 (21), 4138-46.

20. Carlson, K. D.; Johnson, R. E.; Prakash, L.; Prakash, S.; Washington, M. T., Human DNA polymerase kappa forms nonproductive complexes with matched primer termini but not with mismatched primer termini. *Proc Natl Acad Sci U S A* **2006**, 103 (43), 15776-81.

21. Lone, S.; Townson, S. A.; Uljon, S. N.; Johnson, R. E.; Brahma, A.; Nair, D. T.; Prakash, S.; Prakash, L.; Aggarwal, A. K., Human DNA polymerase kappa encircles DNA: implications for mismatch extension and lesion bypass. *Mol Cell* **2007**, 25 (4), 601-14.

22. Pande, P.; Malik, C. K.; Bose, A.; Jasti, V. P.; Basu, A. K., Mutational analysis of the C8-guanine adduct of the environmental carcinogen 3-nitrobenzanthrone in human cells: critical roles of DNA polymerases eta and kappa and Rev1 in error-prone translesion synthesis. *Biochemistry* **2014**, 53 (32), 5323-31.

23. Washington, M. T.; Johnson, R. E.; Prakash, L.; Prakash, S., Human DINB1-encoded DNA polymerase kappa is a promiscuous extender of mispaired primer termini. *Proc Natl Acad Sci U S A* **2002**, 99 (4), 1910-4.

24. Kusumoto, R.; Masutani, C.; Shimmyo, S.; Iwai, S.; Hanaoka, F., DNA binding properties of human DNA polymerase eta: implications for fidelity and polymerase switching of translesion synthesis. *Genes Cells* **2004**, 9 (12), 1139-50.

25. Waters, L. S.; Minesinger, B. K.; Wiltrot, M. E.; D'Souza, S.; Woodruff, R. V.; Walker, G. C., Eukaryotic translesion polymerases and their roles and regulation in DNA damage tolerance. *Microbiol Mol Biol Rev* **2009**, 73 (1), 134-54.

26. Haracska, L.; Prakash, L.; Prakash, S., Role of human DNA polymerase kappa as an extender in translesion synthesis. *Proc Natl Acad Sci U S A* **2002**, 99 (25), 16000-5.

TABLES

Table 1. Sequences of DNA oligonucleotides.

| Oligomer ^{a,b} | DNA Sequence |
|-------------------------------|---|
| Primers | |
| 20-mer | 5'-AACGACGGCCAGTGAATTCG-3' |
| 21-dC | 5'-AACGACGGCCAGTGAATTCGC-3' |
| 21-dG | 5'-AACGACGGCCAGTGAATTCGG-3' |
| 21-dA | 5'-AACGACGGCCAGTGAATTCGA-3' |
| 21-dT | 5'-AACGACGGCCAGTGAATTCGT-3' |
| Templates | |
| 26-mer | 3'-TTGCTGCCGGTCACTTAAGCGCGCCC-5' |
| 26-mer-dG ^{C8-N-ABA} | 3'-TTGCTGCCGGTCACTTAAGC <u>G</u> CGCGCCC-5' |

G indicates the dG^{C8-N-ABA} lesion at the 21st position from the 3' terminus of the template.

Table 2. Kinetic parameters for nucleotide incorporation opposite dG^{C8-N-ABA} or undamaged dG catalyzed by hPolκ.

| dNTP | k_p (s ⁻¹) | $K_{d, dNTP}$ (μM) | $k_p/K_{d, dNTP}$ (μM ⁻¹ s ⁻¹) | Efficiency Ratio ^a | Fidelity ^b | Probability ^c |
|--|--------------------------------|--------------------|---|-------------------------------|------------------------|--------------------------|
| Damaged 20/26-mer-dG^{C8-N-ABA} | | | | | | |
| dCTP | (5.5 ± 1.0) x 10 ⁻¹ | 1710 ± 563 | 3.2 x 10 ⁻⁴ | 116 | - | 43.5 |
| dATP | (1.5 ± 0.1) x 10 ⁻¹ | 504 ± 39 | 3.0 x 10 ⁻⁴ | 2 | 4.8 x 10 ⁻¹ | 40.8 |
| dGTP | (8 ± 2) x 10 ⁻² | 1147 ± 396 | 7.1 x 10 ⁻⁵ | 16 | 1.8 x 10 ⁻¹ | 9.6 |
| dTTP | (1.0 ± 0.1) x 10 ⁻² | 223 ± 73 | 4.5 x 10 ⁻⁵ | 17 | 1.2 x 10 ⁻¹ | 6.1 |
| Undamaged 20/26-mer^d | | | | | | |
| dCTP | 1.7 ± 0.1 | 46 ± 6 | 3.7 x 10 ⁻² | - | - | 94 |
| dATP | (3.2 ± 0.2) x 10 ⁻¹ | 539 ± 71 | 6.0 x 10 ⁻⁴ | - | 1.6 x 10 ⁻² | 1.5 |
| dGTP | (4.1 ± 0.1) x 10 ⁻¹ | 388 ± 29 | 1.1 x 10 ⁻³ | - | 2.9 x 10 ⁻² | 2.8 |
| dTTP | (5.5 ± 0.3) x 10 ⁻¹ | 693 ± 66 | 8.0 x 10 ⁻⁴ | - | 2.1 x 10 ⁻² | 2.0 |

^aCalculated as $(k_p/K_{d, dNTP})_{20/26-mer}/(k_p/K_{d, dNTP})_{20/26-mer-dG^{C8-N-ABA}}$.

^bCalculated as $(k_p/K_{d, dNTP})_{\text{incorrect}}/[(k_p/K_{d, dNTP})_{\text{incorrect}} + (k_p/K_{d, dNTP})_{\text{correct}}]$ for the same DNA substrate.

^cCalculated as $(k_p/K_{d, dNTP})_{20/26-mer-dG^{C8-N-ABA}}/\sum(k_p/K_{d, dNTP})_{20/26-mer-dG^{C8-N-ABA}}$ or

$(k_p/K_{d, dNTP})_{20/26-mer}/\sum(k_p/K_{d, dNTP})_{20/26-mer}$.

^dKinetic parameters for undamaged DNA substrate 20/26-mer are adopted from Table 2 of Sherrer *et al.*¹⁷

Table 3. Kinetic parameters for nucleotide incorporation during the extension of a matched junction base pair dC:dG^{C8-N-ABA} or dC:dG by hPolk.

| dNTP | k_p (s ⁻¹) | $K_{d, dNTP}$ (μM) | $k_p/K_{d, dNTP}$ (μM ⁻¹ s ⁻¹) | Efficiency Ratio ^a | Fidelity ^b | Probability ^c |
|--|--------------------------------|--------------------|---|-------------------------------|------------------------|--------------------------|
| Damaged 21/26-mer-dG^{C8-N-ABA} | | | | | | |
| dGTP | (1.1 ± 0.1) x 10 ⁻² | 770 ± 248 | 1.4 x 10 ⁻⁵ | 786 | - | 70.4 |
| dATP | (3.3 ± 0.2) x 10 ⁻⁴ | 140 ± 41 | 2.4 x 10 ⁻⁶ | 17 | 1.5 x 10 ⁻¹ | 12.1 |
| dCTP | (1.0 ± 0.1) x 10 ⁻³ | 735 ± 123 | 1.4 x 10 ⁻⁶ | 48 | 9.1 x 10 ⁻² | 7.0 |
| dTTP | (1.8 ± 0.1) x 10 ⁻³ | 824 ± 90 | 2.2 x 10 ⁻⁶ | 19 | 1.4 x 10 ⁻¹ | 10.6 |
| Undamaged 21/26-mer^d | | | | | | |
| dGTP | (9.9 ± 0.3) x 10 ⁻¹ | 87 ± 9 | 1.1 x 10 ⁻² | - | - | 98.6 |
| dATP | (2.4 ± 0.2) x 10 ⁻² | 596 ± 121 | 4.0 x 10 ⁻⁵ | - | 3.6 x 10 ⁻³ | 0.36 |
| dCTP | (9 ± 2) x 10 ⁻² | 1343 ± 474 | 6.8 x 10 ⁻⁵ | - | 6.1 x 10 ⁻³ | 0.6 |
| dTTP | (2.5 ± 0.2) x 10 ⁻² | 645 ± 84 | 3.9 x 10 ⁻⁵ | - | 3.5 x 10 ⁻³ | 0.34 |

^aCalculated as $(k_p/K_{d, dNTP})_{21/26-mer}/(k_p/K_{d, dNTP})_{21/26-mer-dG^{C8-N-ABA}}$.

^bCalculated as $(k_p/K_{d, dNTP})_{\text{incorrect}}/[(k_p/K_{d, dNTP})_{\text{incorrect}} + (k_p/K_{d, dNTP})_{\text{correct}}]$ for the same DNA substrate.

^cCalculated as $(k_p/K_{d, dNTP})_{21/26-mer-dG^{C8-N-ABA}}/\sum(k_p/K_{d, dNTP})_{21/26-mer-dG^{C8-N-ABA}}$ or

$(k_p/K_{d, dNTP})_{21/26-mer}/\sum(k_p/K_{d, dNTP})_{21/26-mer}$.

^dKinetic parameters for undamaged DNA substrate 21/26-mer are adopted from Table 2 of Sherrer *et al.*¹⁷

Table 4. Kinetic parameters for the extension of mismatched junction base pairs by hPolk.

| dNTP | k_p (s ⁻¹) | $K_d, dNTP$ (μM) | $k_p/K_d, dNTP$ (μM ⁻¹ s ⁻¹) | Fidelity ^a |
|--|------------------------------|------------------|---|-----------------------|
| Extension of mismatched junction base pair dG:dG^{C8-N-ABA} in 21-dG/26-mer-dG^{C8-N-ABA} | | | | |
| Correct dGTP | (3.1 ± 0.6)x10 ⁻³ | 1155 ± 501 | 2.7 x 10 ⁻⁶ | |
| Incorrect dCTP | (1.1 ± 0.1)x10 ⁻¹ | 1608 ± 331 | 6.8 x 10 ⁻⁵ | 0.96 |
| Extension of mismatched junction base pair dG:dG in 21-dG/26-mer | | | | |
| Correct dGTP | (1.3± 0.2)x10 ⁻³ | 488 ± 174 | 2.7 x 10 ⁻⁶ | |
| Incorrect dCTP | (9.4 ± 0.1)x10 ⁻⁴ | 284 ± 98 | 3.3 x 10 ⁻⁶ | 0.55 |
| Extension of mismatched junction base pair dT:dG^{C8-N-ABA} in 21-dT/26-mer-dG^{C8-N-ABA} | | | | |
| Correct dGTP | (3.2 ± 0.1)x10 ⁻³ | 101 ± 16 | 3.2 x 10 ⁻⁵ | |
| Incorrect dCTP | ND | ND | 3.3 x 10 ⁻⁷ | 1.0x10 ⁻² |
| Extension of mismatched junction base pair dT:dG in 21-dT/26-mer | | | | |
| Correct dGTP | (4.4 ± 0.4)x10 ⁻² | 778 ± 196 | 5.7 x 10 ⁻⁵ | |
| Incorrect dCTP | (1.7 ± 0.1)x10 ⁻³ | 823 ± 101 | 2.1 x 10 ⁻⁶ | 3.6x10 ⁻² |
| Extension of mismatched junction base pair dA:dG^{C8-N-ABA} in 21-dA/26-mer-dG^{C8-N-ABA} | | | | |
| Correct dGTP | (5.7 ± 0.7)x10 ⁻³ | 481 ± 129 | 1.2 x 10 ⁻⁵ | |
| Incorrect dCTP | (3.2 ± 0.1)x10 ⁻³ | 298 ± 23 | 1.1 x 10 ⁻⁵ | 0.48 |
| Extension of mismatched junction base pair dA:dG in 21-dA/26-mer | | | | |
| Correct dGTP | (1.3 ± 0.3)x10 ⁻¹ | 137± 65 | 9.5 x 10 ⁻⁴ | |
| Incorrect dCTP | (9.9 ± 0.1)x10 ⁻³ | 131 ± 62 | 7.6 x 10 ⁻⁵ | 7.4x10 ⁻² |

^aCalculated as $(k_p/K_d, dNTP)_{incorrect}/[(k_p/K_d, dNTP)_{incorrect} + (k_p/K_d, dNTP)_{correct}]$ for the same DNA substrate.

Table 5. Comparison of kinetic parameters for correct nucleotide incorporation by hPol η or hPol κ during dG^{C8-N-ABA} bypass and subsequent extension.

| Parameter | hPol η ^a | hPol κ | Fold-difference ^b |
|---|--------------------------|----------------------|------------------------------|
| dG^{C8-N-ABA} bypass | | | |
| k_p (s ⁻¹) | 1.9 | 0.55 | 3.5 |
| $K_{d,dCTP}$ (μM) | 325 | 1710 | 0.19 |
| $k_p/K_{d,dCTP}$ (μM ⁻¹ s ⁻¹) | 5.8×10^{-3} | 3.2×10^{-4} | 18 |
| Extension of the matched junction base pair dC:dG ^{C8-N-ABA} | | | |
| k_p (s ⁻¹) | 0.8 | 0.01 | 80 |
| $K_{d,dGTP}$ (μM) | 28 | 770 | 0.036 |
| $k_p/K_{d,dGTP}$ (μM ⁻¹ s ⁻¹) | 2.9×10^{-2} | 1.4×10^{-5} | 2071 |

^aKinetic parameters are adopted from Table 4 of Tokarsky *et al.*⁵

^bCalculated as (kinetic parameter)_{hPol η} /(kinetic parameter)_{hPol κ} .

Figure Legends

Figure 1. Metabolic activation of 3-nitrobenzathrone (3-NBA) and formation of a DNA adduct $dG^{C8-N\text{-ABA}}$. Once 3-NBA is nitroreduced to form an intermediate (N-OH-ABA) which is further converted to N-AcO-ABA. N-AcO-ABA then initiates an electrophilic attack on a guanine to generate $dG^{C8-N\text{-ABA}}$.

Figure 2. Determination of kinetic parameters for correct dCTP or incorrect dATP incorporation onto 20/26-mer- $dG^{C8-N\text{-ABA}}$. A pre-incubated solution of 300 nM hPol κ and 30 nM 5'-[^{32}P]-labeled 20/26-mer- $dG^{C8-N\text{-ABA}}$ (A) was mixed with increasing concentrations of dCTP (B) or dATP (C) for various times at 37 °C before being quenched with 0.37 M EDTA. The product concentrations were plotted against reaction times and each time course was fit to Eq. (1) (Materials and Methods) to yield k_{obs} (Figure S2). The k_{obs} values were then plotted against respective concentrations of dCTP (B) or dATP (C) and the plots were fit to Eq. (2) (Materials and Methods) to yield a k_p of $(5.5 \pm 1.0) \times 10^{-1} \text{ s}^{-1}$ and a $K_{d,\text{dCTP}}$ of $1710 \pm 563 \mu\text{M}$ for dCTP incorporation (B) and $(1.5 \pm 0.1) \times 10^{-1} \text{ s}^{-1}$ and $504 \pm 39 \mu\text{M}$ for dATP incorporation (C). **G** in (A) represents the $dG^{C8-N\text{-ABA}}$ lesion.

Figure 3. Extension of primer-terminal matched or mismatched junction base pairs by hPol κ . A preincubated solution of hPol κ (300 nM) and 5'-[^{32}P]-labeled DNA (30 nM) was rapidly mixed with a specific dNTP (500 μM) at 37 °C for indicated times before being quenched by 0.37 M EDTA. Unreacted substrate (21-mer) was shown at the bottom of each gel picture with extended

products located sequentially above the unreacted substrate. Reaction time intervals (minutes) were indicated below each lane.

FIGURES

Figure 1

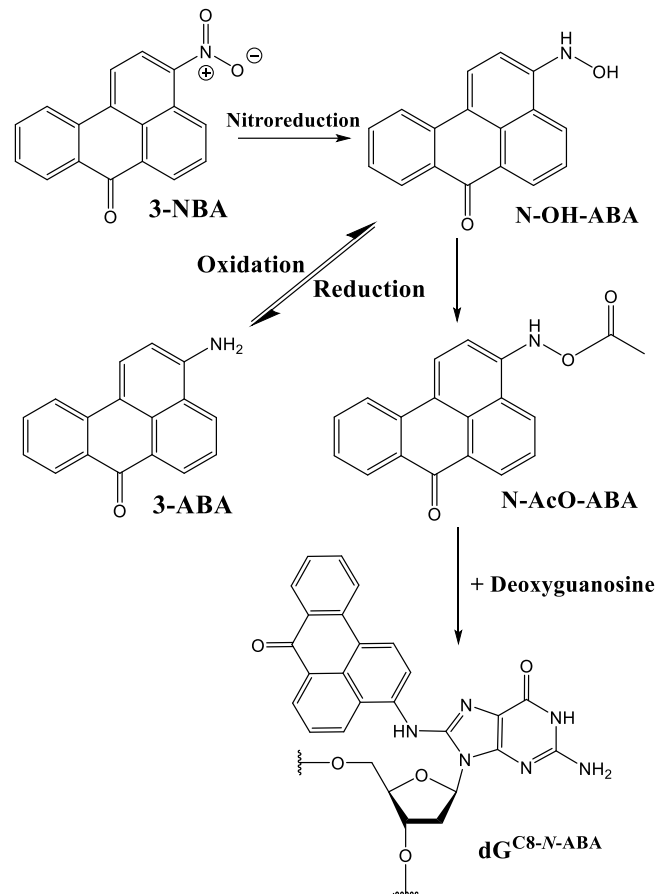
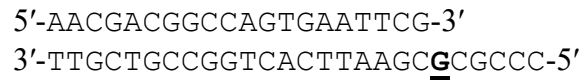
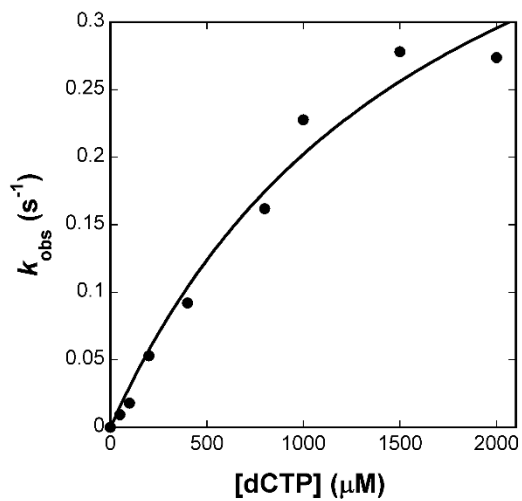


Figure 2

A



B



C

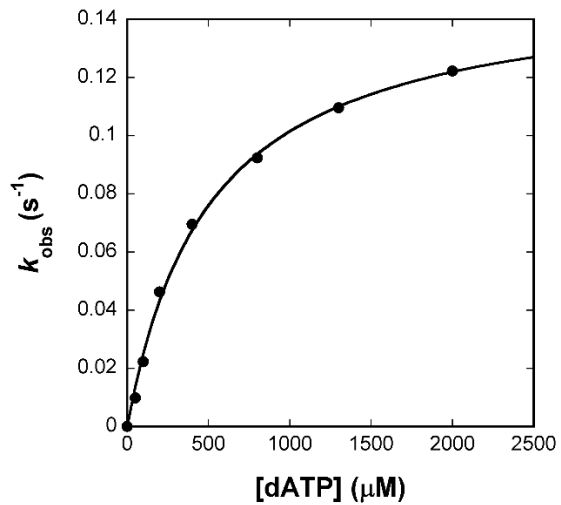


Figure 3

